

OVERLORD: Ultimate Scaling of DataLoader for Multi-Source Large Foundation Model Training

Juntao Zhao^{1,2,◦}, Qi Lu^{1,◦}, Wei Jia^{1,◦,†}, Borui Wan^{1,2}, Lei Zuo¹, Junda Feng¹, Jianyu Jiang¹, Yangruai Chen¹, Shuaishuai Cao¹, Jialing He¹, Kaihua Jiang¹, Yuanzhe Hu¹, Shibiao Nong¹, Yanghua Peng^{1,†}, Haibin Lin^{1,†}, Xin Liu^{1,†}, Chuan Wu^{2,†}

¹ByteDance Seed, ²The University of Hong Kong

◦Equal Contribution, †Corresponding authors

Abstract

Modern frameworks for training large foundation models (LFMs) employ dataloaders in a data-parallel manner, with each loader processing a disjoint subset of training data. Under multisource preprocessing, two fundamental challenges exist. First, due to the quadratic computational complexity of the attention operator, the non-uniform sample distribution over data-parallel ranks leads to significant workload imbalance among dataloaders, degrading the training efficiency. Second, supporting diverse data sources requires per-dataset file access states that are redundantly replicated across parallel loaders, consuming excessive memory. This also hinders dynamic data mixing (e.g., curriculum learning) and causes redundant access/memory overhead in hybrid parallelism.

We present OVERLORD, an industrial-grade distributed data loading architecture for LFMs, with four innovations: (1) Disaggregated data preprocessing via role-specific actors (Source Loaders/Data Constructors) to eliminate source and parallelism redundant data access and ensure multisource scalability. (2) Centralized and declarative data plane for elastic multisource orchestration, such as long-short context, multimodality, and curriculum learning. (3) Multi-level auto-partitioning and scaling mechanism for source loaders under heterogeneous preprocessing costs. (4) Shadow loaders with differential checkpointing for fault recovery without workflow interruption. Deployed on production clusters scaling to multi-thousand GPUs, OVERLORD achieves: (1) 4.5× end-to-end training throughput improvement, (2) 13.5× reduction in CPU memory usage.

Date: May 20, 2025

1 Introduction

The rise of large language and vision models, a.k.a. large foundation models (LFM), has propelled numerous downstream applications to achieve remarkable performance. Training LFMs faces major challenges on model efficiency and data efficiency. Model efficiency is related to effectively distributing a massive model parameters among GPUs to maximize resource utilization and reduce resource waste. Significant advances in training framework design [29, 43, 45, 49, 65] and novel parallelism paradigms [26, 36, 37] have been made, largely addressing model efficiency. Data efficiency, on the other hand, ensures that sufficient resources (e.g., CPU cores and DRAM) are allocated to the data preprocessing pipeline to avoid input data stalls during training and underutilization of valuable GPU hours.

Modern training frameworks partition the global training batch across data-parallel dataloaders, with each loader tasked with loading and preprocessing its assigned data subset. Specifically, LFM training data stems from diverse multilingual and multimodal sources, such as text (Wikipedia, Common Crawl [19]), images (ImageNet [15], LAION [46]), and domain-specific collections [17]. To meet the needs of LFM training, engineers typically depend on ad-hoc scripts to blend these datasets into *data mixtures* [7, 17, 51], which combine data sources at specified ratios for different use cases. Although some prior works [6, 21, 22, 41, 52, 63] have delved into data efficiency in model training, multisource preprocessing in LFM introduces unique challenges.

Multisource Data Orchestration. Under non-uniform sample distributions from diverse sources, the quadratic computational complexity of the attention operator [54] introduces significant workload imbalances. For example, a complete sequence composed of 30-token and 70-token subsequences incurs 16% more computation than two 50-token subsequences. These imbalances are manifested both intra- and inter-microbatch [62], creating stragglers over data parallel ranks, exacerbating pipeline bubbles over pipeline stages, and prolonging training time. The data imbalance is compounded by non-uniform data distribution across modality modules. In vision-language models (VLMs) [57–59], for instance, image encoders process raw pixels while language backbones operate on fused image-patch and text tokens. In that way, modality data within a training batch offers different workload across modules within the VLM.

Multisource Scalability. Constructing data mixtures from massive sources introduces fundamental memory constraints. First, each dataloader worker process maintains independent data file access states via dedicated per-source resources: separate socket connections, schemas, metadata structures, and I/O buffers (e.g., Parquet Row Group [4]). This architecture imposes linear memory overhead growth concerning the number of data sources—a critical limitation given that modern LFM training incorporates hundreds of data sources. Second, practitioners perform multimodal *transformations* (JPEG/RGB conversion, video keyframe extraction [5, 18]) at runtime to avoid inflated storage (up to $200\times$ for OCR). Such heavyweight processing necessitates vertical scaling of worker numbers to prevent data stalls, and dramatically increases the memory pressure of the dataloader. Disparities across data sources exacerbate the situation. For instance, audio processing requires $4\times$ more computation per output token than image decoding and $300\times$ more than text tokenization. Analogous heterogeneity also occurs in unimodal contexts through variable resolutions in images/videos. This forces the loader worker number to be sized for the data source with the largest preprocessing cost, creating severe resource over-provision.

Additionally, modern LFMs require data mixtures aggregated from diverse sources under user-defined schedules [17, 51] or dynamically adapted to runtime training metrics (e.g., loss, entropy [1, 28]). For instance, curriculum learning [50] follows an "easy-to-hard" progression, gradually increasing the proportion of challenging samples from difficult datasets. Such scenarios demand a data preprocessing framework that can express arbitrary mixing schedules and scale efficiently with evolving dataset preprocessing costs. Additionally, LFM training is coupled with hybrid model parallelism, where multiple ranks within a parallelism group often share ephemeral preprocessed data. In context parallelism (CP) groups, ranks process the same batch but different sequence partitions; with pipeline parallelism (PP), the first stage requires the full batch while others possess metadata for communication. Without coordination, each rank has to manage a dedicated dataloader instance, incurring redundant storage and preprocessing costs. The input system should be able to reconcile the hybrid parallelism to remove redundancy.

Current dataloaders struggle to meet the demands of Large Foundation Model (LFM) training. Mainstream frameworks like Megatron-LM [43], DDP [35], FSDP [65], and MegaScale [29] adopt an SPMD paradigm, colocating dataloaders with training processes. This simplifies programming but hinders global batch orchestration across devices. Existing input data load-balancing solutions (e.g., TensorFlow’s `tf.data` [41], Ray Data [38]) offer limited APIs that cannot model data source disparities (e.g. Modality) or hybrid parallelisms. Remote dataloader systems (e.g., Cachew [21], `tf.data.service` [6], Pecan [22], FastFlow [52]) offload preprocessing to CPU workers but overlook multisource memory scalability—each worker loads hundreds of unpartitioned sources, leading to combinatorial memory growth and inefficiencies for heterogeneous multisource data [22, 52]. We owe the deficiency of existing solutions to their coupled design for data preparation and data delivery.

To address these limitations, we present OVERLORD, a disaggregated data processing framework designed

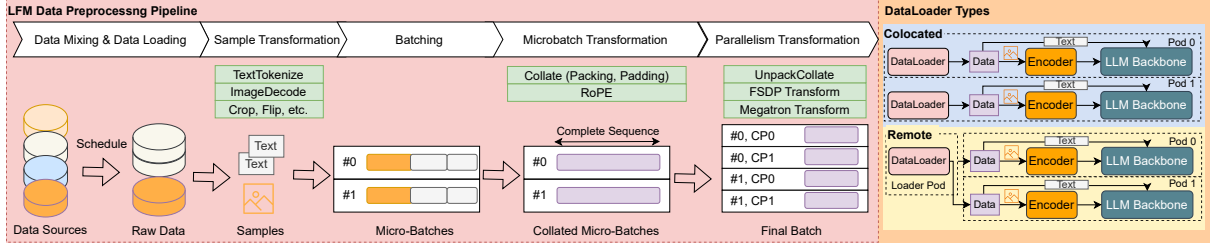


Figure 1 Left: Dataflow of Vision Language Model pretraining. Right: Two types of dataloaders.

for large-scale foundation model workloads that require two core capabilities: global data orchestration and multisource scalability. The key insights behind OVERLORD are the disaggregation of the multisource data preparation and the final delivery. It decomposes multisource preprocessing into specialized roles—dedicated Source Loaders for sample-level transformations (e.g., JPEG decoding) and aggregating Data Constructors for batch-level operations (e.g., tensor padding, splitting)—to eliminate redundant source-level and parallelism-related data access, also mitigating connectivity overhead. It introduces a programmable data plane with DGraph, a stateful dataflow graph tracking dependencies and lineage for each data source, and ClientPlaceTree, a hierarchical topology model enabling hybrid parallelism-aware scheduling, to support declarative cross-module multisource data strategy definition. It employs source auto-partitioning and mixture-driven auto-scaling to dynamically optimize worker allocation for heterogeneous preprocessing demands, and ensures continuous data service via hot standby "shadow" loaders and differential checkpointing with adaptive state persistence frequencies, minimizing GPU idle time during failures or resharding.

Our contributions are summarized below:

- ▷ **Disaggregated multisource preprocessing architecture:** We design a distributed actor-model-based preprocessing pipeline that eliminates redundant data access and memory overhead in LFM multisource data preprocessing (Sec. 3)
- ▷ **Declarative Data Orchestration:** The DGraph and ClientPlaceTree abstractions enable hybrid parallelism-aware data orchestration with minimal user coding effort (Sec. 4).
- ▷ **Adaptive Multisource Scaling:** We introduce scalable algorithms that dynamically optimize CPU utilization for data preprocessing based on heterogeneous source preprocessing costs and evolving data mixing ratios (Sec. 5).
- ▷ **Uninterrupted Data Feeding:** OVERLORD sustains continuous data delivery to training processes without requiring intervention during runtime adjustments (Sec. 6).
- ▷ Production results show that OVERLORD improves multimodal VLM training throughput by $4.5\times$ and reduces CPU usage by $13.5\times$ versus data parallel baselines. It sustains GPU busy time even during elasticity events (Sec. 7).

2 Background and Motivation

We depict and analyze the production input data preprocessing pipeline for a Visual-Understanding-Language Model (VLM). Our analysis reveals the challenges and opportunities inherent in the data processing framework for LFM training.

2.1 LFM Input Data Preprocessing

As shown in Fig. 1, data from different datasets is mixed and loaded from cloud or distributed file systems, such as Amazon S3 [2] and HDFS [3]. On-the-fly transformations are conducted to convert input training samples into tensors that are ready for training. This "last-mile" data conversion is performed by online data processing frameworks, commonly referred to as dataloaders, such as the PyTorch DataLoader [44].

Data Mixing and Data Loading. In LFM training, samples from different data sources are combined in proportions to formulate a *data mixture* [51], resulting in a comprehensive, inclusive training corpus. The mixing ratio adjustment can be performed in a scheduled way, like with curriculum learning paradigms in reinforcement learning [50] and warmup [33] and staged training [51] techniques, or in a dynamic manner, where the sampling weights of the data sources vary in response to evolving training status (such as loss and entropy [10, 28]). The dataloader utilizes the sampling ratios of the mixing schedule to load data proportionally from different datasets (sources).

Sample Transformations are applied to each data sample, converting the data format and improving the data quality [6, 22, 64]. For example, text tokenization and image decoding convert raw text and image data into trainable representations (e.g., text tokens and normalized RGB tensors). Similarly, the *crop* transformation standardizes image dimensions by cropping and resizing inputs to a fixed resolution.

Microbatch Transformation. After batching sampled data into microbatches, microbatch transformations collate samples to standardize the input shape. Packing merges fragmented subsequences into complete sequences with segmented masks [14, 31]. Padding aligns variable-length sequences by adding dummy tokens [14, 31]. Finally, positional embedding transformations like RoPE [11] are applied to obtain complete context information.

Parallelism Transformation. To effectively parallelize LFM training with increasing data and model sizes, hybrid parallelism strategies have been adopted. Hybrid parallelisms significantly influence how model training consumes training data. In data parallelism (DP) [13, 34, 48], microbatches are partitioned across training devices, and each device independently processes its local data using its model replica. Context parallelism (CP) [30, 37] partitions and scatters the input sequence; each device within a CP group consumes a part of the input sequence. Tensor parallelism (TP) [43] performs intra-operator partitioning, with each device within a TP group receiving the same input. Pipeline parallelism (PP) [25, 42] segments the model layers into stages, where only the first stage (PP0) obtain all microbatches, and intermediate results are exchanged between consecutive stages through peer-to-peer (P2P) communications. These replication and partitioning relationships between input data and hybrid parallelism schemes are encoded as parallelism transformations, applied after the microbatch transformation to ensure each client receives the correct input data.

Multimodal LFMs [24, 62] further complicate the input data processing pipeline with **heterogeneous collocation**. Multimodal LFMs are composed of more than one module (encoders, backbone, etc.), and each module may process different parts of the input data and employ different hybrid parallelism schemes. For example, a VLM can employ pure data parallelism for the vision encoder (e.g., ViT [16]) training and 4D (PP-DP-CP-TP) parallelism for LLM backbone (e.g., LLaMA [17, 39]) training. The parallelism difference for different data within a batch requires careful parallelism transformation programming.

2.2 Colocated and Remote Dataloader

As shown on the right of Fig. 1, conventional ML training frameworks (e.g., Torch [44]) typically colocate the dataloader with the training process. We observe that mainstream LFM training frameworks, such as Megatron-LM [43], DDP [35], FSDP [65], and MegaScale [29], still adhere to this practice. One advantage of colocated dataloaders is that they share the same sharding configuration (e.g., data parallelism) and CPU resources with the training process, eliminating the need for additional configuration. However, their rigid loader setup limits their ability to right-sizing resources like CPU and DRAM for efficient data processing.

Remote dataloaders, exemplified by Meta’s Data Processing Service (DPP) [63] and Google’s tf.data service [6], offload data preprocessing to disaggregated CPU workers over the accelerator nodes. This architecture enables elastic scaling of data preprocessing throughput. Recent studies—Cachew [21], FastFlow [52], Cedar [64], and Pecan [22]—further optimize resource efficiency by orchestrating heterogeneous CPU resources across local and remote nodes. Nonetheless, all the existing dataloader systems fail to meet the new demands of LFM training, to be detailed in the following.

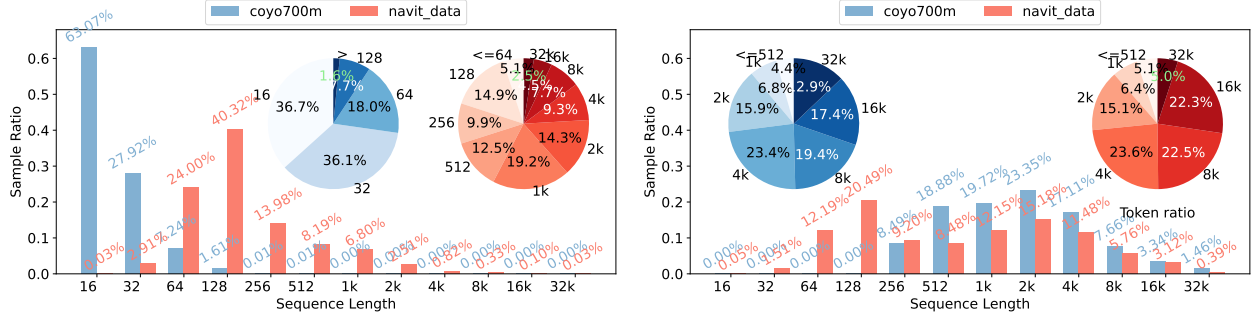


Figure 2 Token distribution in the two source datasets. Left: Text token. Right: Image token.

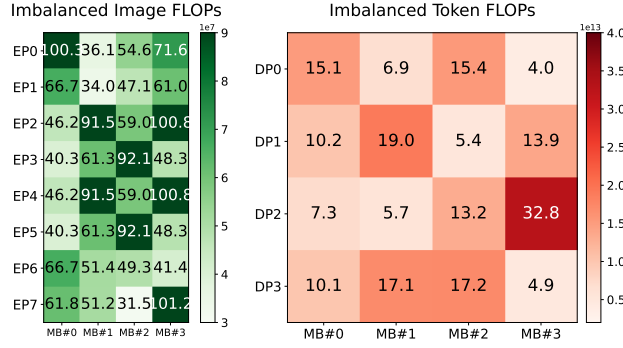


Figure 3 Computational imbalance across microbatches. DPx denotes the data parallel rank x , and $MB\#x$ represents the x -th microbatch.

2.3 LFM Data Preprocessing Requirements

Multisource Data Orchestration. Data scheduling remains consistently necessary due to data heterogeneity under sophisticated training parallelism schemes. VLMs construct training samples by interleaving encoded images and text tokens. Each input sample comprises an image-text pair: images are split into patches and encoded into tokens via a visual encoder, while text labels are tokenized separately. These token streams are then interleaved to form complete training sequences. Fig. 2 shows the token distributions in the open-source *coyo700M* [9] dataset and our production *navit_data* dataset, where "text" represents text tokens, and "image" indicates the number of 16×16 (*coyo*) and 14×14 (*navit*) image patches [14]. Both distributions are significantly skewed. In *coyo700M*, 98.23% of samples contain text sequences ≤ 64 tokens, while the top 1.62% of longer sequences (> 64 tokens) account for 9.3% of all tokens. Similar skewness occurs in image subsequences. Such skewness manifests two critical computational challenges:

(1) *Intra-module imbalance.* The quadratic time complexity of the attention operation ($O(l^2)$ with l as sequence length) [12] induces a significant computational disparity between microbatches containing subsequences of varying length. Fig. 3 shows this disparity, where we benchmark an 8-card VLM training trial, colocating encoders and the backbone, with EP degree of 8 for the encoder's data parallel training, and $DP = 4/TP = 2$ for the LLM backbone's hybrid parallelism. The maximum microbatch FLOPs observed are $3.2 \times$ and $6.9 \times$ larger than the minimum for images and complete sequences, respectively.

(2) *Inter-module imbalance.* Input data distributions can vary significantly across modules. As shown in Fig. 3, even for the same microbatch, there exists a substantial divergence in the token distributions between raw image patches and the final collated sequence. Given the heterogeneous parallelisms of colocated modules on the same GPU, Data Parallel rank #3 (DP3) for the LLM backbone corresponds to Encoder Parallel ranks 6 and 7 (EP6, EP7). The computational complexity of image tokens across microbatch #3 are balanced between every two consecutive DP ranks ($140e7$); however, DP3's MB#3 workload (4.9×10^{13} FLOPs) is significantly smaller than DP2's MB#3 (32.8×10^{13} FLOPs), indicating a severe imbalance. Moreover, when

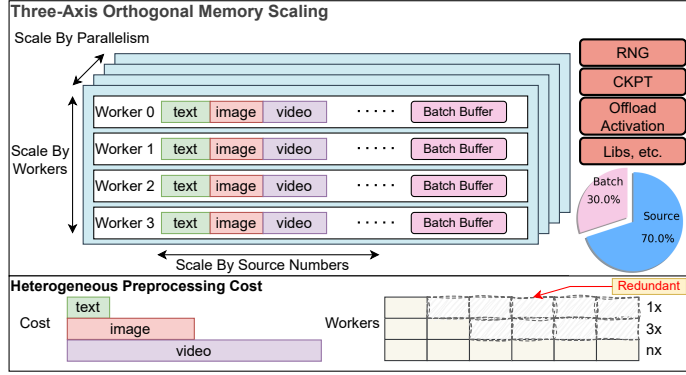


Figure 4 Orthogonal memory scaling and heterogeneous source dataset preprocessing costs.

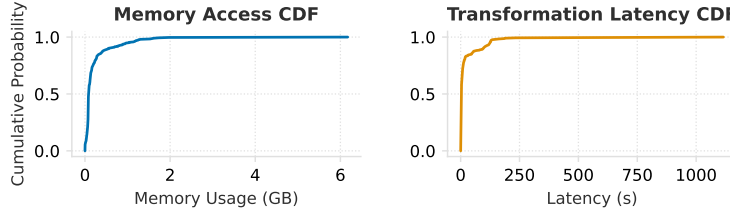


Figure 5 Cumulative distribution function (CDF) of 100 samples across production source datasets. Left: file access states memory (GB). Right: transformation latency (s).

considering only the encoder data parallel ranks for MB#3, the FLOPs across DP ranks remain unbalanced and necessitate adjustment. To address this, data scheduling strategies should be tailored distinctly for different modules to homogenize their workloads.

Additionally, existing solutions often leverage all-to-all communication protocols at the model layer to aggregate information for load balancing input batches (e.g., [62]). However, this approach introduces four fundamental challenges: increased activation size, elevated communication overhead, scalability bottlenecks, and tight coupling of load balancing logic with model-layer codebases, which risks contaminating the core computation workflow. We argue that load-time data orchestration presents a compelling alternative: an LFM data preprocessing system should proactively balance data from heterogeneous sources across modules before model ingestion.

Multisource Scalability. The multisource nature of LFM training data exerts substantial memory pressure on the preprocessing pipeline. As demonstrated in Fig. 4, our production-scale LFM training trials reveal that when the per-DP training batch size remains moderate, the memory footprint of replicated file access states for data sources constitutes over 70% of the total memory consumption during data preprocessing. This multisource memory overhead arises from two orthogonal scaling dimensions.

(1) *Source Scaling.* Modern LFMs achieve task generality through source datasets aggregated from diverse domains [7, 17, 60]. In production systems, training jobs process hundreds to thousands of distinct source files that collectively define the global data mixture. Each file introduces a fixed per-source memory overhead. For instance, practitioners commonly store training data in columnar formats such as Parquet [4], which optimize compression ratios and access locality through feature grouping [66]. Parquet files partition data into row groups (512MB–1GB storage units [4]). During reads, a client first establishes a dedicated socket to the file, loads metadata (e.g., footers, schema information) into memory, and executes queries over row groups using buffers [61]. This design inherently leads to linear memory overhead scaling: independent file states (sockets, metadata, buffers) per source cause memory usage to grow proportionally with the source number.

(2) *Worker Scaling.* To prevent GPU idling, practitioners must optimally size dataloader worker processes to

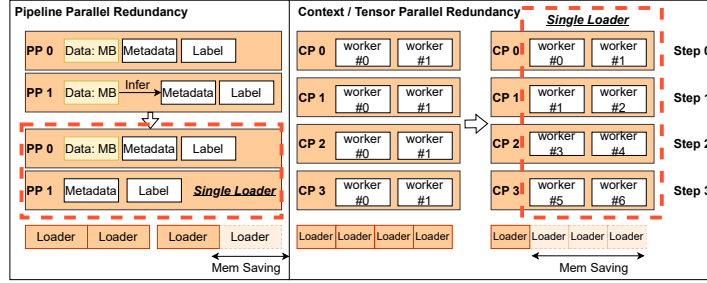


Figure 6 Parallelism Redundancy for Loader Instances.

match data transformation bottlenecks. Each worker process maintains its execution context and prefetch buffer [44], and thus the memory consumption scales with the number of workers. This issue is exacerbated by transformation time heterogeneity across modalities. For instance, text tokenization is lightweight, whereas image decoding (e.g., RGB conversion via PIL [53]) and video processing (e.g., keyframe extraction [5]) are computationally intensive. Even for the data of the same modality, e.g., images, patches [14] for variable-resolution images introduce order-of-magnitude cost differences. As a result, transformation latencies exhibit severe skewness across sources, as shown in Fig. 5. Critically, when faced with multiple data sources, loader workers must dynamically resize to match the throughput of the slowest transformation pipeline (Fig. 4). This prevents vibrating feeding rates that could otherwise introduce GPU idle time. However, this approach forces dataloaders to scale workers based on worst-case latency demands, necessitating over-provisioning for faster pipelines.

These observations underscore the need for multisource-scalable preprocessing design. An effective solution must address both (1) horizontal memory growth due to increasing sources and (2) vertical memory amplification from worker scaling under heterogeneous, time-varying transformation latency.

2.4 Challenges For Preprocessing Requirements

To address the above requirements, efficient design of an LFM data preprocessing framework faces the following challenges.

First, the dynamic data mixing of LFM training alters data source sampling ratios at runtime, necessitating the data orchestration panel to express and adapt with runtime data source sampling patterns. Additionally, it mandates that multisource scalability solutions not only support arbitrary mixing strategies but also automatically adjust the source mixing ratios as training progresses, given that per-source transformation latency evolves non-uniformly over time.

Next, as elaborated in Sec. 2.1, ranks in context parallelism and pipeline parallelism require only partial input data for model execution. In the absence of coordination, each rank independently instantiates a full dataloader to load complete batches for data partitioning and metadata retrieval (Fig. 6). This leads to redundant loader instances that scale with the number of CP/PP ranks, exacerbating memory overhead (Fig. 4). To mitigate this, the framework must tightly integrate data orchestration with hybrid parallelism, eliminating redundant data access and memory occupation by sharing ephemeral, parallelism-aware preprocessed input training data across ranks.

Finally, LFM training may dynamically adjust GPU allocations at runtime—elastic scaling (addition/deletion), redeployment, resharding, or failure events [55, 56]—which requires persistent data services to maintain stable data feeding speeds. These scenarios demand built-in mechanisms in the data preprocessing framework for resilient connectivity and fault tolerance to ensure uninterrupted data delivery.

2.5 Opportunities

Current dataloaders suffer from significant limitations. Mainstream input systems, such as tf.data [41], Ray Data [38], and PyTorch DataLoader [44], cannot reconcile multisource input data under hybrid parallelism.

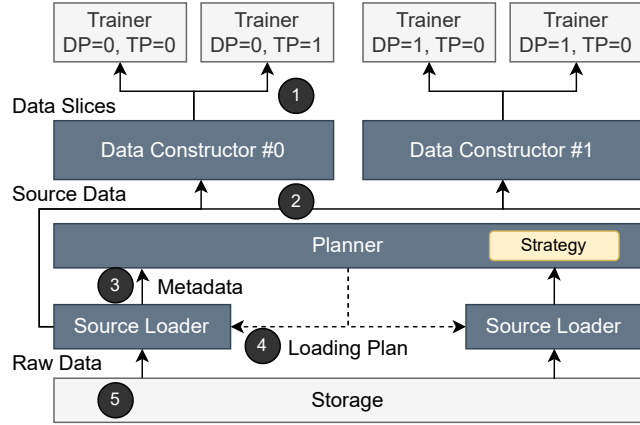


Figure 7 Architecture of OVERLORD. Solid lines denote data paths; dashed lines represent control paths.

This forces redundant data access and manual handling of multi-source scheduling and mixing logic, leading to high development complexity. Remote dataloaders such as Pecan and FastFlow [22, 52] focus on scaling resources for specific data transformation, but still suffer from linearly increasing memory consumption with data sources and pipeline workers, resulting in unsustainable costs. Colocated dataloaders share memory with training processes, which are even more memory-intensive: as illustrated in Fig. 4, during LFM training, they compete for memory with quite a few memory consumers (e.g. RNG states, checkpoints [56], etc.) The inflated data batch buffer is also redundantly duplicated with parallel loader workers. Additionally, existing systems lack resilience for large-scale distributed workloads. Failures in data workers or network partitions can halt entire training runs, necessitating manual intervention and costly restarts.

OVERLORD addresses these issues with four architectural innovations. It employs an actor-model architecture to split preprocessing into Source Loaders and Data Constructors, improving scalability and eliminating redundant access in hybrid parallelism and multisource setups. A centralized data plane with declarative interfaces simplifies cross-module data scheduling. Multilevel source auto-partitioning and mixture-driven scaling optimize resource use. Finally, state isolation enables shadow dataloaders and differential checkpointing for failure recovery without interrupting dataflow.

3 OVERLORD Overview

OVERLORD is a data preprocessing framework for LFM training designed for unified orchestration and resource-efficient delivery of multisource training data. As shown in Fig. 7, OVERLORD employs a hierarchical architecture with three core components: *Source Loader*, which continuously ingests data from assigned source while applying sample transformations; *Data Constructor*, which generates data samples for a specified DP rank by aggregating Source Loader outputs and applying microbatch and parallelism transformations; *Planner*, which orchestrates system-wide behavior through (1) aggregating metadata from Source Loaders and generating the loading plans, and (2) adjusting data mixing ratios and triggering Source Loader autoscaling based on workload fluctuations and cost-efficiency targets.

Deployment. Components of OVERLORD are fully deployed on the CPU. During bootstrap, OVERLORD provisions Data Constructors and trainer clients according to trainer device topology and auto-partitions source datasets into multiple Source Loaders during instantiation (Sec. 5) based on their journalized profiling results. The Planner initiates an orchestration strategy to be implemented by the user via OVERLORD’s programming model (Sec. 4), enabling policy-driven control over dataflows.

Workflow. The runtime data preprocessing follows a lazy execution model. Each component (Data Constructor,

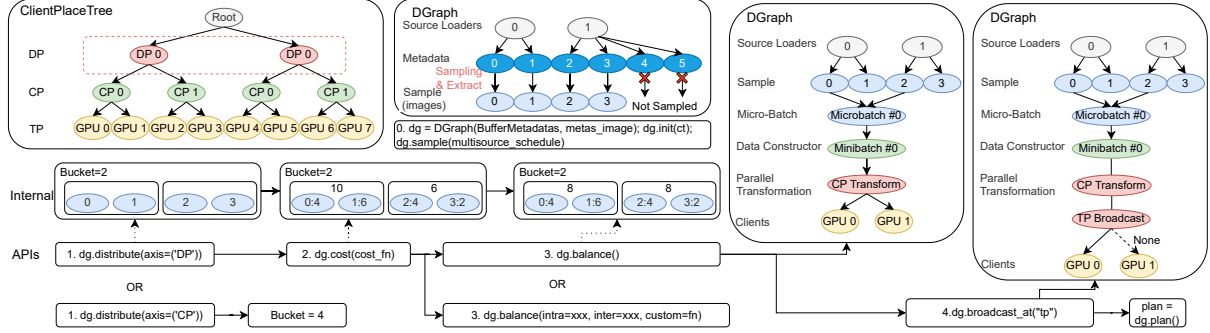


Figure 8 Balance multisource data on devices with hybrid parallelism (DP=2, CP=2, TP=2).

Source Loader, Planner) maintains its own task queue. The workflow proceeds as: ❶ A trainer-side client requests data from its Data Constructor. ❷ The Data Constructor triggers positional data fetches from all Source Loaders. ❸ Source Loaders consult the Planner to generate new loading plans. ❹ The Planner synthesizes new plans by collecting buffer metadata (e.g., sample indices, source signatures, sequence length) from Source Loaders. Finalized plans direct Source Loaders to prepare samples, pop them from the read buffers, and stage them in queues. ❺ Source Loader reads new samples from the distributed storage and populates them into the buffer.

Design Rationale. In OVERLORD, data constructors act as data sinks for ranks in each data parallel (DP) group, enabling seamless data sharing among ranks that consume the same batch. Ranks in the same context parallelism group can generate sequence partitions concurrently from identical batches, while pipeline parallelism stages requiring only metadata can exclude unnecessary data or label items from the shared data dictionary. Meanwhile, source loaders are dedicated to their sources, thus removing the redundancy of file access states.

4 Data Orchestration Panel

4.1 Abstraction

Existing dataloader frameworks like `tf.data.service` [6] provides distributed execution APIs but lacks native abstractions for two critical requirements: (1) multisource representation for data within the same batch, and (2) trainer-side hybrid parallelism scheme integration (e.g., 4D parallelism, PP, DP, CP, and TP). These gaps complicate unified implementation of multisource and cross-module data orchestration.

To address these limitations, OVERLORD introduces two core abstractions: *DGraph* for source-aware data transition state tracking and *ClientPlaceTree* for parallelism strategy resolution, as exemplified in Fig. 8.

DGraph is a state-tracking dataflow graph that models the lifecycle of training samples through explicit producer-consumer relationships. It is initialized by binding data samples to their respective Source Loaders. Upon plan generation, it associates each sample to its target Data Constructor. Each node in *DGraph* represents a training sample in a specific processing state, with directed acyclic edges encoding either data transformations or logical dependencies (e.g., minibatch grouping). Edges may be null if no state mutation occurs. *DGraph* operates on lightweight metadata and delivers two core advantages: *Unified multisource representation*, that allows creation of multiple source-specific graphs (e.g., test-image pair or text data from a specific source) from the same shared data dict through selective metadata specification; *Orchestration transparency*, which visualizes dataflow states, dependencies, and transformations via directed acyclic edges in an interpretable way.

ClientPlaceTree is a logical representation of the trainer device mesh. It provides a clear view of how data is accessed by trainers at different ranks and in different communication groups while abstracting details such as device memory capacities from users. Presenting the topology as a tree allows for easy modifications to the structure and automates the generation of parallelism transformation.

4.2 Primitives

As illustrated in Fig. 8, OVERLORD initializes its data orchestration primitives using buffer metadata collected from Source Loader buffers and a *ClientPlaceTree* encoding GPU allocations. Orchestration begins by specifying the modality metadata to create *DGraph*, enabling OVERLORD to encode either single or multiple modalities for load balancing. This modular approach is particularly valuable for models like VLMs, where multiple modules within the same process handle different data modalities at runtime, allowing separate specifications of balancing and transformation strategies. We further define several primitives for *DGraph* that can express most of our existing data orchestration strategies.

`mix(schedule)` enables real-time source mixing through scheduled sampling. Users define a multisource schedule that generates the sampling weight of source datasets for each training step (at epoch, step, or substep granularity [47]), determining the probabilistic selection of source data batches. Only sampled data participates in subsequent orchestration.

`distribute(axis, group_size)` specifies the axis along which data distribution occurs. This enables straightforward implementation of diverse partitioning strategies: (1) `axis='DP'` partitions data into minibatches across data-parallel groups;

(2) `axis='CP'` treats $DP \times CP$ GPUs as uniform consumers for hybrid data parallelism [20]; (3) `axis='WORLD'` distributes data across all ranks for the encoder module in VLMs with world-wide data parallelism. Once the distribution axis is selected, OVERLORD automatically determines the parallelism transformations (e.g., CP transformations). The primitive creates n buckets corresponding to nodes at the specified axis level in the *ClientPlaceTree* hierarchy. When `group_size` is provided, the effective bucket count scales to $\lceil \frac{n}{\text{group_size}} \rceil$, and samples are balanced within subgroups instead, reducing coordination overhead in super large clusters.

`cost(costfn)` registers a cost function that estimates compute and memory overhead from sample metadata. Costs are automatically propagated to subsequent `balance` operations. For text pretraining, sequence length can serve as a data load and HBM occupation metric. For VLMs, the number of images or image sequence length [14] is a suitable encoder cost model, while token count quadratic functions capture backbone resource usage.

`balance(method, *)` balances samples based on their computed costs. It further divides buckets into m bins, where m is the number of microbatches, and then applies the specified balancing method to distribute samples among these bins. We provide two candidate balancing methods: `greedybinpacking` and `karmarkar-karp` [8]. These can be applied at both intra-microbatch (bin) and inter-microbatch (bucket) levels [62], or interleaving. To keep the global batch unchanged, users may optionally disable intra-microbatch reordering via configuration. User-defined balancing strategies (e.g., Zig-Zag) can also be implemented with framework’s extension API.

`broadcast_at(target_dim)` indicates to *DGraph* that a broadcast operation exists on the trainer side along the specified dimension. For example, when TP0 broadcasts data to all TP ranks, this directive informs the Data Constructor to exclude $tp > 0$ clients from data fetching. This mechanism optimizes communication by preventing redundant data access.

`plan()` dynamically generates optimized data-loading plans. Based on the plans, the Source Loader operates according to the plan to execute data mixing and scheduling, and then forwards prepared samples to the Data Constructor. The Data Constructor handles microbatch assembly and performs microbatch and parallelism transformations.

In addition to these primitives, we offer low-level programming interfaces with better flexibility, including `plan_raw`, `loader_do_plan`, `constructor_do_plan` and `summary_buffer`, which enable the user to program Planner, Source Loaders, and Data Constructor data consuming policies directly.

4.3 Use Cases

As shown in Fig. 9, our APIs simplify the development of data orchestration strategies through a three-stage workflow: Extract, Orchestrate, and Finalize. To showcase the broad applicability and adaptability of our programming model, we analyze two representative use cases. In the scenario of unimodal long-short sequence 4D-parallel training across data-parallel ranks, taking data D , and *ClientPlaceTree* C as inputs, our framework

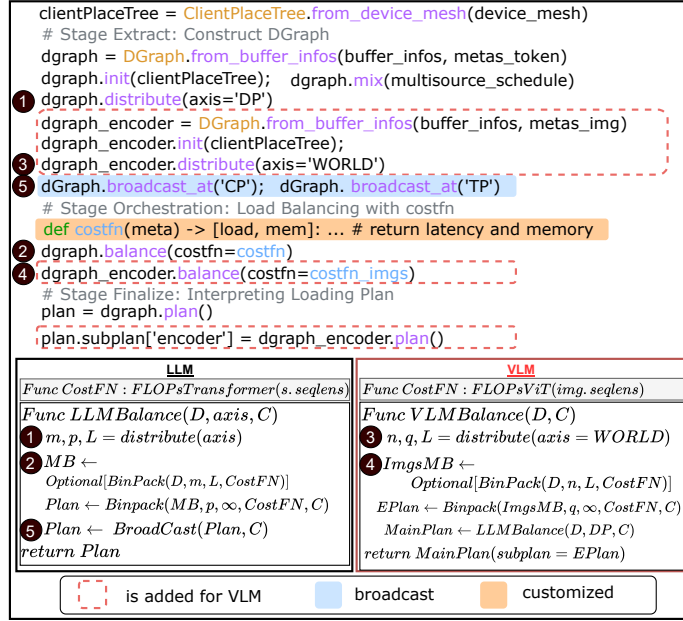


Figure 9 Strategy implementation of unimodal long-short sequence and multimodal vision language model pretraining task. Users can adapt to new training tasks by adding new lines and customizing limited functions.

achieves intra-module balancing (LLMBalance) using only seven lines of code, incorporating a cost model (*CostFN*). ① First, it distributes data along the DP axis to determine the number of data-parallel partitions, per-DP microbatches, and memory limit L , ② Next, it generates a resource consumption plan through balancing with greedy binpack. ⑤ If broadcast operations are included, the consumers are tailored. For the VLM setup, an inter-module balancing strategy is implemented with just five additional lines of code. The image DGraph is inferred using the same buffer but different metadata. We first distribute ③ and balance ④ images with data parallel, then combine with *LLMBalance* to perform global balancing across the modules. These concise implementations demonstrate the expressiveness and versatility of our framework in diverse LFM training environments.

5 MultiSource Loader Autoscaling

The AutoScaler in OVERLORD addresses two core multisource scalability challenges: (1) partitioning and balancing heterogeneous preprocessing workloads and memory footprints across data sources, and (2) scaling of dynamic source mixing ratios. As shown in Fig. 10, OVERLORD employs a two-phase approach: ① **Offline Source Auto-Partitioning**: Sources are partitioned with loader parallel schemes to obtain Source Loader configurations. ② **Online Mixture-Driven Scaling**: At runtime, OVERLORD dynamically scales and reshards Source Loaders in response to mixing ratio shifts, keeping low data preprocessing cost and resource efficiency under fluctuating demand.

5.1 Source Auto-Partitioning

We first analyze the parallelism schemes for partitioning the Source Loader, then introduce our scalable solution and elaborate its underlying rationale.

Dataloader Parallelism Schemes. The end-to-end preprocessing cost is modeled as a tuple (P, T, M) , where P denotes transformation latency, T represents orchestration and data transfer overhead, and M signifies memory footprint, comprising batch buffer (M_b) and per-source file access states (M_d). As shown in Fig. 10, we analyze three parallelism strategies to distribute costs across loaders: (1) *Worker Parallel* amortizes

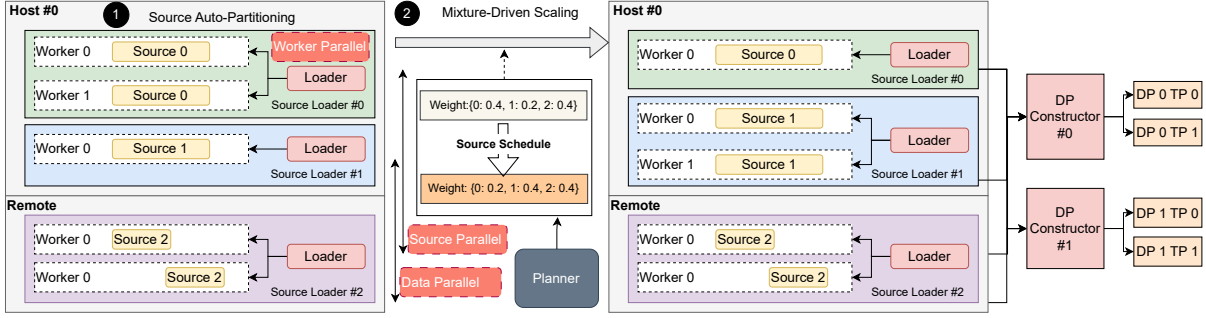


Figure 10 Two-Phase AutoScaling. (1) Offline Source Auto-Partitioning, (2) Online Mixture-Driven Scaling.

P by staggering execution. Parallel workers in a loader initiate transformation $n - 1$ steps ahead of their successors, where n is the total worker count), enabling concurrent execution. (2) *Source Parallel* reduces M_d by partitioning data sources across multiple Source Loaders. Each loader worker maintains fewer file access states, decreasing memory pressure from metadata and I/O channels. (3) *Data Parallel* reduces P and M_b by sharding training data across loaders [6, 22], whose degree is bounded by the batch size.

MultiLevel Source Partition Given heterogeneous transformation costs $\{P_1, \dots, P_k\}$ and memory footprints $\{M_1, \dots, M_k\}$ across k data sources, we partition each source by default into multiple data-parallel actors, each containing worker-parallel workers with varying counts. The partition algorithm proceeds in three stages. (1) *Source Clustering*: We first sort all data sources in descending order of transformation cost P_k and cluster them into G source clusters. Empirical analysis shows that a cluster size of 4 achieves optimal performance in most scenarios. (2) *Resource Level Construction*: Using the ratio of mean transformation costs between the smallest and largest clusters, we estimate the number of workers for each source within a cluster. Available resources are calculated by subtracting resource allocations for the Data Constructor (estimated via fixed batch size) and Planner from total system resources. These available resources are divided by the total number of workers to form worker resource blocks. To prevent invalid data parallelism for global batches and physical pod resource overcommitment, we set upper bounds w_{src} (per-source worker limit) and w_{actor} (per-actor worker limit), and then generate actor counts (loader data parallelism degree) and worker counts for each resource level. (3) *Configuration Generation*: We derive resource configurations for each source within clusters. When memory resources are insufficient for M_k , we adjust the number of source actors to satisfy memory constraints.

5.2 Mixture-Driven Scaling

A key architectural advantage of OVERLORD is the Planner’s centralized control over data mixture sampling, providing global visibility into cross-source mixing ratios (Fig. 7). This enables predictive autoscaling: as sampling weights evolve, the Planner dynamically adjusts Source Loader resources based on projected demand. When a source’s moving-average sampling weight exceeds a threshold for consecutive intervals, the Planner triggers the AutoScaler to: (1) create new Source Loader actors, (2) reshard data partitions live, and (3) integrate the scaled actors into the plan generation. Idle resources are reclaimed inversely under declining demand.

5.3 Design Rationale

We default to assigning one source per Source Loader actor, trading moderate communication for resource overhead, for two reasons. First, arbitrary mixing schedules complicate source grouping: maintaining stochastic consistency is challenging when sources in the same group exhibit divergent weight trajectories. Second, dedicated per-source actors eliminate most scaling needs from mixture changes, stabilizing feeding rates. While grouping remains suitable for static schedules, users can enable it during source clustering (1).

Our focus on horizontal scaling via actor/worker counts utilizes underutilized CPU resources co-located with accelerators. Empirical studies [23] and our trials show 75% idle auxiliary CPU capacity under static

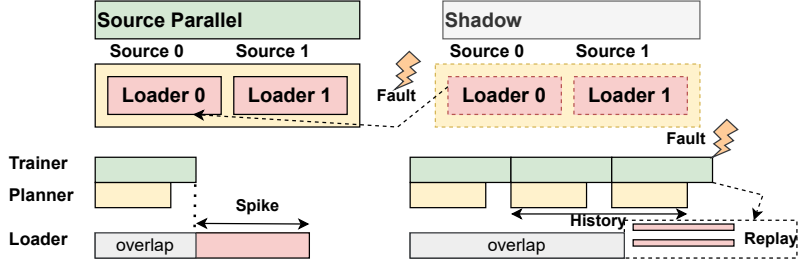


Figure 11 Loader Failure Recovery: Shadow Loader, Replay with Differential Checkpointing Intervals.

allocations; actor-level management enables finer-grained control.

6 Large-Scale Deployment

OVERLORD is implemented atop Ray [40], with 8763 lines of Python code. We discuss practical issues and solutions when deploying OVERLORD at scale.

6.1 Non-Interrupted Fault Tolerance

Here, we discuss the non-interrupted fault tolerance mechanisms for each component illustrated in Fig. 7.

Planner / Constructor. The Planner and Data Constructor ensure fault tolerance through continuous state checkpointing to a persistent store. During failures, training proceeds uninterrupted if client prefetch buffers retain sufficient data; otherwise, a trainer-side barrier halts batch requests until recovery. Upon recovery, these actors reconstruct the state from the latest checkpoint. The Data Constructor then prefetches new loading plans using trainer-reported positions to synchronize with the current training state.

Source Loader. OVERLORD leverages Shadow Loaders—hot-standby replicas that maintain synchronized states with active loaders. As shown in Fig. 11, upon detecting a loader failure, the Planner seamlessly promotes a warm-standby Shadow Loader to active status, ensuring uninterrupted data delivery. We also employ replay to mitigate the higher checkpoint latency of the loader due to its large data buffer. Instead of maintaining a consistent journaling rate, the loader’s checkpoint frequency is set lower than that of the Planner to gain a store window.

6.2 Deployment

We employ the following deployment tricks. **(1) Deploy as a sidecar service.** We deploy OVERLORD as a sidecar to isolate resources and utilize idle CPU/memory in accelerator pods [32]. OVERLORD only proactively scales remote resources for remote resources when sidecar resources become insufficient. **(2) Transformation Reordering.** Inspired by Pecan [22], we defer image decoding to the data constructor stage, reducing communication data size. **(3) Selective Broadcasting.** To tackle the high synchronization overhead of trainer-side client barriers in large clusters, we propose bottom-up selective broadcasting on ClientPlaceTree, e.g., broadcast a tensor at TP, CP, or DP group. This increases memory and communication costs but reduces the number of synchronized clients.

7 Evaluation

We evaluate OVERLORD by quantifying its improvements in orchestration performance and multi-source loading efficiency under large-scale deployment.

7.1 Experiment Setup

Models. We evaluate OVERLORD on Visual-Language Models (VLMs) using both dense and sparse Large Language Models (LLMs) as backbone, in combination with the Vision Transformer (ViT) [16] as the image

Table 1 Model configurations.

	Model	#Layers	#Heads	Hidden Size
Encoder	ViT - 1B	39	16	1408
	ViT - 2B	48	16	1664
LLM	Llama - 12B	45	36	4608
	tMoE - 25B	42	16	2048 (topk = 2)
	Mixtral - 8×7B	32	32	4096 (topk = 2)

encoder. The details of the models are given in Table 1. For the dense model, we select the Llama3 series [17]. For sparse models (Mixture-of-Experts - MoE), we choose the Mixtral series [27]. We also evaluate one production MoE model named tMoE.

Workloads. We use two dataset groups (Fig. 2 in Sec. 2.3), namely *coyo700m* and *navit_data*, consisting of 5 and 306 sources, respectively. We test OVERLORD across various batch sizes, context lengths, and GPU numbers. We further scaled up to 4096 GPUs to benchmark scalability in Appendix B.

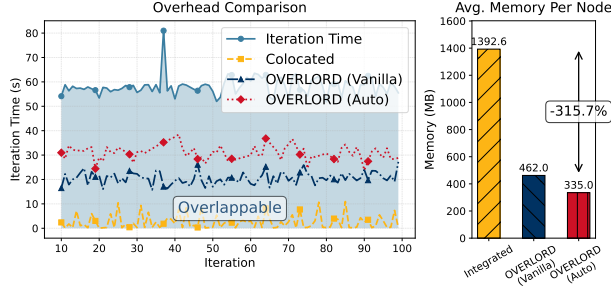
Metrics. We use training throughput, measured in tokens per second (tokens/s), as our primary metric. The results are collected after the initial warmup phases and averaged over 100 training iterations. We also show elapsed iteration time (s) and average memory usage per node (GB). We don’t count the memory occupation of shadow loaders to make a fair comparison.

Baselines. For performance evaluation, we gauge the orchestration efficiency of our solution in three scenarios: (1) Vanilla, a system without any data scheduling; (2) Backbone balance, which implements inter-microbatch load balancing exclusively on the LLM backbone; (3) Hybrid balance, which combines interleaved balancing (directly balancing sampled images across ranks) for the encoder with the backbone balance, as described in Fig. 9. We do not perform intra-microbatch balancing for the LLM backbone. For system components evaluation, we comparing OVERLORD with the Colocated DataLoader. We also benchmark OVERLORD-Vanilla, acting with pure actor-model data preprocessing without data source partition and shadow loader. We do not compare with scaling solutions like Pecan [22], tf.data.service [6], and Ray Data [38], as these focus on speeding up data transformation and can be smoothly integrated into our framework.

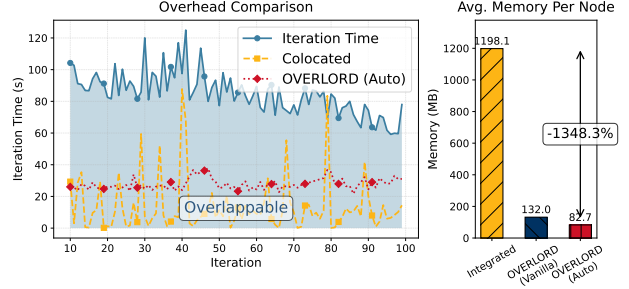
Testbed. We conduct our experiments on a training cluster composed of multiple nodes, each equipped with 16× NVIDIA L20 GPUs (48GB) and 1.8TB of host DRAM. We employ the sidecar mode to launch isolated containers on the host, allocating half of the available CPU cores and memory resources to the resource pool for Ray scheduling. The entire training cluster is interconnected via InfiniBand, with HDFS as the storage backend.

7.2 Data Preprocessing Architecture Evaluation

We demonstrate resource savings achieved by OVERLORD using the Llama-12B + ViT-2B combination on 288 and 576 GPUs, with a batch size of 72 for each GPU. We sample 100 sources from the *navit_data* dataset to construct *navit-100*. Due to host memory limitations of the Colocated Loader, 100 sources are served by 4 loader workers, while a single loader worker serves 306 sources. To utilize the GPU resources and avoid HBM OOM (out of memory), we size the backbone layer number to fit the model into the GPU memory. We measure the memory usage at each node and calculate the average memory per node. As illustrated in Fig. 12, OVERLORD achieves significant resource savings compared to the colocated loader, with up to 13.5× reduction. Although OVERLORD introduces additional data fetch overhead by offloading local loading to remote locations, this overhead can be fully overlapped with the model’s training forward pass. Consequently, it does not impact training performance. In particular, for the 576-GPU setup, the colocated loader experiences severe fluctuations in data fetch costs due to insufficient workers. In contrast, OVERLORD manages to maintain a consistent data transmission rate by better using the resources at each node. Specifically, OVERLORD-auto reduces resource occupation by eliminating resource redundancy per loader worker. However, it outperforms OVERLORD-Vanilla only in the 576-GPU scenario, not in the



(a) 288 Cards. TP=4, PP=4, 32k, 8 layers.



(b) 576 Cards. TP=4, PP=4, CP=4, 32k, 16 layers.

Figure 12 Memory usage and data fetch time comparison. The overhead under the elapsed training iteration time can be fully overlapped. In the 576-GPU case, OVERLORD-Vanilla failed to continuously feed the data.

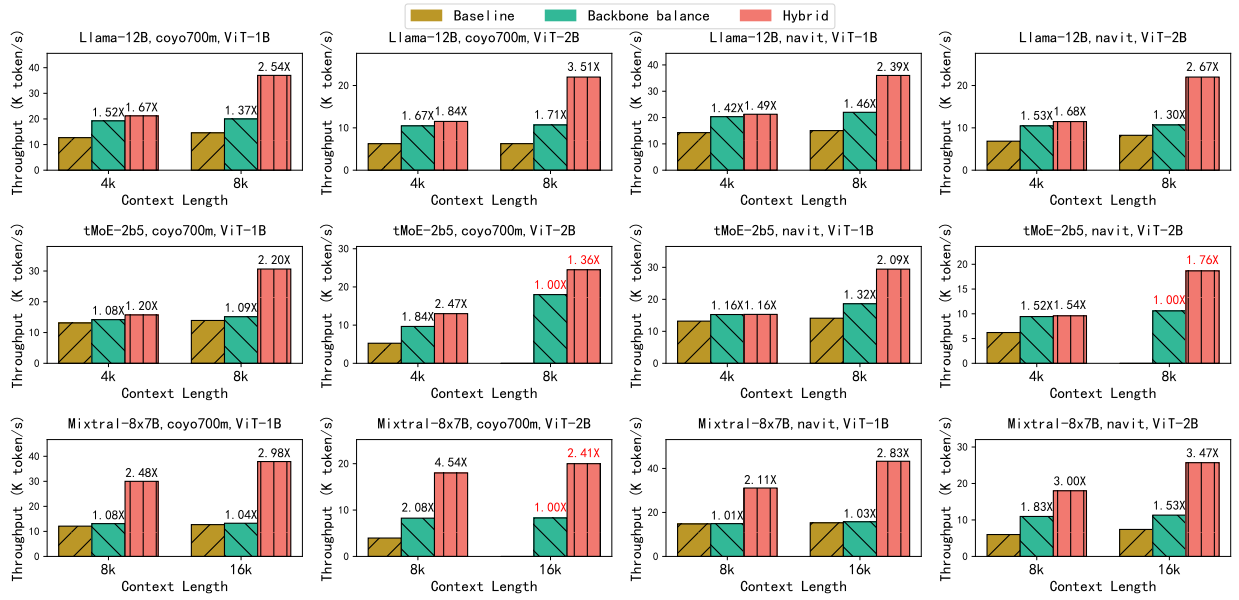


Figure 13 End-to-end orchestration performance across varying context lengths, dataset groups, and model sizes.

288-GPU case. This is because auto-source partition requires more running actors and additional resources, making it more suitable for large-scale deployments.

7.3 Orchestration Evaluation

The results of the end-to-end orchestration performance are shown in Fig. 13. Compared to the non-scheduling baseline, our approach achieves up to $4.54\times$ (average $1.77\times$) throughput improvement. The following key observations are made.

Larger Context Lengths Amplify Heterogeneity Increasing context lengths consistently improve training throughput, validating the effectiveness of the sequence-packing decision. However, longer contexts also introduce greater in-batch heterogeneity. Our balancing strategy capitalizes on this property, yielding higher gains: 4k contexts achieve an average speedup of $1.71\times$, 8k contexts yield $2.63\times$, and 16k contexts reach $3.09\times$. In the absence of load balancing, peak activation memory can induce OOM errors, as empirically observed in our ViT-2B experiments. The results also validate the necessity of our load-time balancing strategy, which also mitigates the excessive memory overhead caused by all-to-all collective communication.

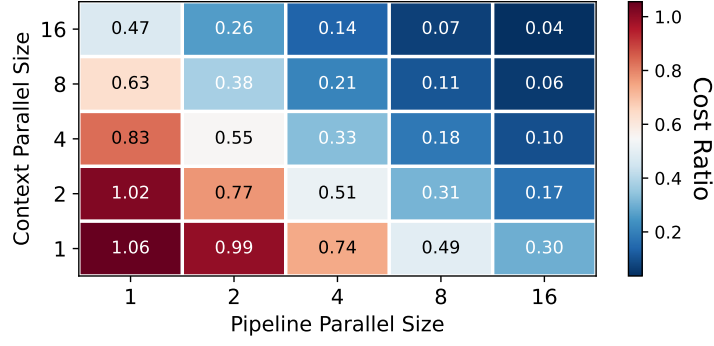


Figure 14 Simulated Memory Cost Ratio of OVERLORD compared with Colocated Loader. OVERLORD achieves substantial resource savings in most cases.

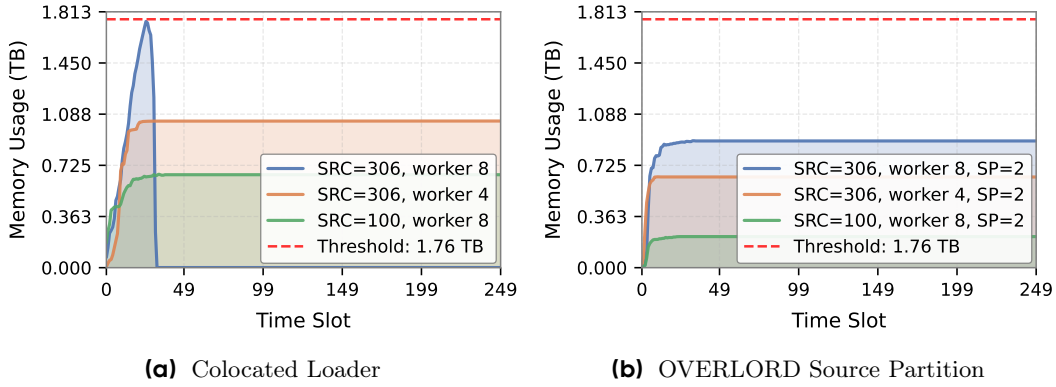


Figure 15 Effect of Source Parallelism on Host Memory Occupation. OVERLORD partition sources with DP size 2 (SP=2).

Dataset Characteristics Influence Gains Fig. 2 shows that *coyo700m* contains shorter text subsequences than *navit_data*, leading to greater heterogeneity for image computation with equivalent context lengths. This manifests in higher speedups with hybrid balancer: *coyo700m* achieves $2.48\times$ average (up to $4.54\times$) versus *navit_data*’s $2.42\times$ average (up to $3.47\times$). For 4k contexts with *navit_data*, encoder balancing provides limited benefit as small context length results in few samples inside a batch, which offers very limited scheduling space.

Encoder Scaling Affects Strategy Efficacy Hybrid balancing (encoder + backbone) outperforms encoder-only strategies more significantly with larger encoders. For Llama-12B, ViT-2B shows $1.58\times$ gain versus ViT-1B’s $1.41\times$ under hybrid balancing. This relationship reverses for larger contexts: ViT-1B achieves up to $2.86\times$ speedup over vanilla orchestration in Mixtral configurations, suggesting that context length interacts non-linearly with the encoder scale, given our current strategy.

7.4 Ablation Study

Parallelism Redundancy Removal We quantify the redundancy reduction of OVERLORD using a dry-run approach to generate dummy data loading jobs and profile memory usage to create a *simulated backend*. Memory occupation is benchmarked under BS=512, 512 nodes and 4 workers, without data source partitioning. As shown in Fig. 14, OVERLORD introduces marginal overhead at low parallelism levels due to its data constructor’s buffering requirements. However, with increasing context and pipeline parallelism levels, memory efficiency gains become significant. Ablation studies for worker count, cluster size, and batch size are given in Appendix A.

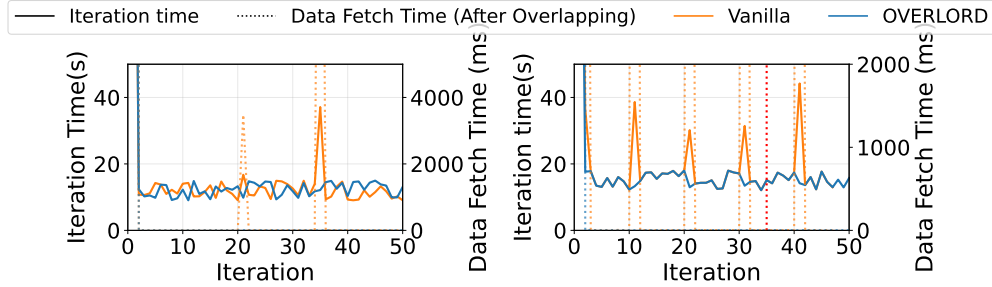


Figure 16 Non-Interrupted Fault Tolerance. Left: Planner; Right: Loader. When a fault is injected, the data fetch time spikes.

Source Redundancy Removal We further evaluate the efficacy of source parallelism (partitioning). Using a cluster configuration of $TP=16$ and $DP=2$, we disable the trainer to isolate data loading performance and benchmark *navit_100* and *navit_data* datasets across varying worker counts. OVERLORD is configured to uniformly partition data sources across DP ranks with a batch size of 32 and context length of 32k. Fig. 15a reveals that *navit_100* exhibits significantly lower memory footprint than *navit_data* under identical worker configurations. Notably, as shown in Fig. 15b, source partitioning yields substantial reductions in memory overhead.

7.5 Fault-Tolerance

We evaluate the fault tolerance mechanisms for both Planner and Source Loader through systematic failure injection experiments. For the Planner, we characterize checkpoint recovery performance under varying prefetch buffer sizes (2 and 4 units) by simulating training jobs with 64 concurrent loaders and injecting Planner failures every 15 iterations, starting after the initial 5 warm-up steps. As shown in Fig. 16, each failure injection causes a transient spike in data fetch latency. With sufficient prefetch buffer capacity, the system effectively overlaps Planner reload overhead, enabling seamless recovery. Conversely, undersized buffers result in persistent spikes in both data fetch latency and total training time. To assess loader fault tolerance, we simulate failures by randomly terminating 5–10 loaders at step 35. The results in Fig. 16 demonstrate that the shadow loader mechanism achieves immediate failure recovery, maintaining uninterrupted data delivery to the training pipeline.

8 Conclusion

OVERLORD tackles the challenge of scalable multi-source data preprocessing and orchestration for large foundation model training. The actor-model preprocessing framework eradicates source and parallelism redundancy in multisource data loading, ensuring scalable preprocessing for LFM training jobs. The declarative data plane simplifies the programming of intricate cross-module, multi-source data scheduling and mixture sampling strategies. Leveraging source autoscaling, we partition and organize heterogeneous sources effectively. Fault-tolerant mechanisms guarantee resilient data delivery, exploiting shadow loaders and differential checkpointing. Experiments show that OVERLORD outperforms state-of-the-art baselines significantly in terms of throughput and resource efficiency, while maintaining scalability and robustness.

References

- [1] Alon Albalak, Liangming Pan, Colin Raffel, and William Yang Wang. Efficient online data mixing for language model pre-training, 2023. URL <https://arxiv.org/abs/2312.02406>.
- [2] Amazon Web Services. Amazon S3 (simple storage service), 2025. URL https://docs.aws.amazon.com/zh_cn/emr/latest/ReleaseGuide/emr-hbase-s3.html. Accessed: 2025-03-22.
- [3] Apache Software Foundation. Hadoop distributed file system (hdfs), 2025. URL https://docs.aws.amazon.com/zh_cn/emr/latest/ReleaseGuide/emr-encryption-tdehdfs.html. Accessed: 2025-03-22.
- [4] Apache Software Foundation. Apache parquet documentation: File format configurations, 2025. URL <https://parquet.apache.org/docs/file-format/configurations/>. Accessed: 2025-03-22.
- [5] Milan K Asha Paul, Jeyaraman Kavitha, and P Arockia Jansi Rani. Key-frame extraction techniques: A review. *Recent Patents on Computer Science*, 11(1):3–16, 2018.
- [6] Andrew Audibert, Yang Chen, Dan Graur, Ana Klimovic, Jiří Šimša, and Chandramohan A. Thekkath. tf.data service: A case for disaggregating ml input data processing. In *Proceedings of the 2023 ACM Symposium on Cloud Computing, SoCC '23*, page 358–375, 2023.
- [7] Xiao Bi, Deli Chen, Guanting Chen, Shanhuang Chen, Damai Dai, Chengqi Deng, Honghui Ding, Kai Dong, Qiushi Du, Zhe Fu, et al. Deepseek llm: Scaling open-source language models with longtermism. *arXiv preprint arXiv:2401.02954*, 2024.
- [8] S. Boettcher and S. Mertens. Analysis of the karmarkar-karp differencing algorithm. *The European Physical Journal B*, 65(1):131–140, August 2008. ISSN 1434-6036. doi: 10.1140/epjb/e2008-00320-9. URL <http://dx.doi.org/10.1140/epjb/e2008-00320-9>.
- [9] Minwoo Byeon, Beomhee Park, Haecheon Kim, Sungjun Lee, Woonhyuk Baek, and Saehoon Kim. Coyo-700m: Image-text pair dataset. <https://github.com/kakaobrain/coyo-dataset>, 2022.
- [10] Mayee F. Chen, Nicholas Roberts, Kush Bhatia, Jue Wang, Ce Zhang, Frederic Sala, and Christopher Ré. Skill-it! a data-driven skills framework for understanding and training language models, 2023. URL <https://arxiv.org/abs/2307.14430>.
- [11] Shouyuan Chen, Sherman Wong, Liangjian Chen, and Yuandong Tian. Extending context window of large language models via positional interpolation, 2023. URL <https://arxiv.org/abs/2306.15595>.
- [12] Tri Dao, Daniel Y. Fu, Stefano Ermon, Atri Rudra, and Christopher Ré. FlashAttention: Fast and memory-efficient exact attention with IO-awareness. In *Advances in Neural Information Processing Systems (NeurIPS)*, 2022.
- [13] Jeffrey Dean, Greg Corrado, Rajat Monga, Kai Chen, Matthieu Devin, Mark Mao, Marc' aurelio Ranzato, Andrew Senior, Paul Tucker, Ke Yang, Quoc Le, and Andrew Ng. Large scale distributed deep networks. In F. Pereira, C.J. Burges, L. Bottou, and K.Q. Weinberger, editors, *Advances in Neural Information Processing Systems*, volume 25. Curran Associates, Inc., 2012. URL https://proceedings.neurips.cc/paper_files/paper/2012/file/6aca97005c68f1206823815f66102863-Paper.pdf.
- [14] Mostafa Dehghani, Basil Mustafa, Josip Djolonga, Jonathan Heek, Matthias Minderer, Mathilde Caron, Andreas Steiner, Joan Puigcerver, Robert Geirhos, Ibrahim M Alabdulmohsin, Avital Oliver, Piotr Padlewski, Alexey Gritsenko, Mario Lucic, and Neil Houlsby. Patch n' pack: Navit, a vision transformer for any aspect ratio and resolution. In A. Oh, T. Naumann, A. Globerson, K. Saenko, M. Hardt, and S. Levine, editors, *Advances in Neural Information Processing Systems*, volume 36, pages 2252–2274. Curran Associates, Inc., 2023. URL https://proceedings.neurips.cc/paper_files/paper/2023/file/06ea400b9b7cfce6428ec27a371632eb-Paper-Conference.pdf.
- [15] Jia Deng, Wei Dong, Richard Socher, Li-Jia Li, Kai Li, and Li Fei-Fei. Imagenet: A large-scale hierarchical image database. In *2009 IEEE Conference on Computer Vision and Pattern Recognition*, pages 248–255, 2009.
- [16] Alexey Dosovitskiy, Lucas Beyer, Alexander Kolesnikov, Dirk Weissenborn, Xiaohua Zhai, Thomas Unterthiner, Mostafa Dehghani, Matthias Minderer, Georg Heigold, Sylvain Gelly, Jakob Uszkoreit, and Neil Houlsby. An image is worth 16x16 words: Transformers for image recognition at scale, 2021.
- [17] Abhimanyu Dubey, Abhinav Jauhri, Abhinav Pandey, Abhishek Kadian, Ahmad Al-Dahle, Aiesha Letman, Akhil Mathur, Alan Schelten, Amy Yang, Angela Fan, et al. The llama 3 herd of models. *arXiv preprint arXiv:2407.21783*, 2024.

- [18] Haoqi Fan, Tullie Murrell, Heng Wang, Kalyan Vasudev Alwala, Yanghao Li, Yilei Li, Bo Xiong, Nikhila Ravi, Meng Li, Haichuan Yang, Jitendra Malik, Ross Girshick, Matt Feiszli, Aaron Adcock, Wan-Yen Lo, and Christoph Feichtenhofer. Pytorchvideo: A deep learning library for video understanding. In Proceedings of the 29th ACM International Conference on Multimedia, MM '21, page 3783–3786, New York, NY, USA, 2021. Association for Computing Machinery. ISBN 9781450386517. doi: 10.1145/3474085.3478329. URL <https://doi.org/10.1145/3474085.3478329>.
- [19] Common Crawl Foundation. Common crawl. <https://commoncrawl.org>, 2014.
- [20] Hao Ge, Junda Feng, Qi Huang, Fangcheng Fu, Xiaonan Nie, Lei Zuo, Haibin Lin, Bin Cui, and Xin Liu. Bytescale: Efficient scaling of llm training with a 2048k context length on more than 12,000 gpus, 2025. URL <https://arxiv.org/abs/2502.21231>.
- [21] Dan Graur, Damien Aymon, Dan Kluser, Tanguy Albrici, Chandramohan A Thekkath, and Ana Klimovic. Cachew: Machine learning input data processing as a service. In 2022 USENIX Annual Technical Conference (USENIX ATC 22), pages 689–706, 2022.
- [22] Dan Graur, Oto Mraz, Muyu Li, Sepehr Pourghannad, Chandramohan A. Thekkath, and Ana Klimovic. Pecan: Cost-Efficient ML data preprocessing with automatic transformation ordering and hybrid placement. In 2024 USENIX Annual Technical Conference (USENIX ATC 24), pages 649–665, Santa Clara, CA, July 2024. USENIX Association. ISBN 978-1-939133-41-0. URL <https://www.usenix.org/conference/atc24/presentation/graur>.
- [23] Qinghao Hu, Zhisheng Ye, Zerui Wang, Guoteng Wang, Meng Zhang, Qiaoling Chen, Peng Sun, Dahua Lin, Xiaolin Wang, Yingwei Luo, Yonggang Wen, and Tianwei Zhang. Characterization of large language model development in the datacenter, 2024. URL <https://arxiv.org/abs/2403.07648>.
- [24] Jun Huang, Zhen Zhang, Shuai Zheng, Feng Qin, and Yida Wang. {DISTMM}: Accelerating distributed multimodal model training. In 21st USENIX Symposium on Networked Systems Design and Implementation (NSDI 24), pages 1157–1171, 2024.
- [25] Yanping Huang, Youlong Cheng, Ankur Bapna, Orhan Firat, Dehao Chen, Mia Chen, Hyoungho Lee, Jiquan Ngiam, Quoc V Le, Yonghui Wu, et al. Gpipe: Efficient training of giant neural networks using pipeline parallelism. Advances in neural information processing systems, 32, 2019.
- [26] Sam Ade Jacobs, Masahiro Tanaka, Chengming Zhang, Minjia Zhang, Leon Song, Samyam Rajbhandari, and Yuxiong He. DeepSpeed Ulysses: System optimizations for enabling training of extreme long sequence transformer models. arXiv preprint arXiv:2309.14509, 2023.
- [27] Albert Q. Jiang, Alexandre Sablayrolles, Antoine Roux, Arthur Mensch, Blanche Savary, Chris Bamford, Devendra Singh Chaplot, Diego de las Casas, Emma Bou Hanna, Florian Bressand, Gianna Lengyel, Guillaume Bour, Guillaume Lample, L  lio Renard Lavaud, Lucile Saulnier, Marie-Anne Lachaux, Pierre Stock, Sandeep Subramanian, Sophia Yang, Szymon Antoniak, Teven Le Scao, Th  ophile Gerv  t, Thibaut Lavril, Thomas Wang, Timoth  e Lacroix, and William El Sayed. Mixtral of experts, 2024. URL <https://arxiv.org/abs/2401.04088>.
- [28] Yiding Jiang, Allan Zhou, Zhili Feng, Sadhika Malladi, and J. Zico Kolter. Adaptive data optimization: Dynamic sample selection with scaling laws, 2024. URL <https://arxiv.org/abs/2410.11820>.
- [29] Ziheng Jiang, Haibin Lin, Yinmin Zhong, Qi Huang, Yangrui Chen, Zhi Zhang, Yanghua Peng, Xiang Li, Cong Xie, Shibiao Nong, et al. {MegaScale}: Scaling large language model training to more than 10,000 {GPUs}. In 21st USENIX Symposium on Networked Systems Design and Implementation (NSDI 24), pages 745–760, 2024.
- [30] Vijay Korthikanti, Jared Casper, Sangkug Lym, Lawrence McAfee, Michael Andersch, Mohammad Shoeybi, and Bryan Catanzaro. Reducing activation recomputation in large transformer models, 2022. URL <https://arxiv.org/abs/2205.05198>.
- [31] Mario Michael Krell, Matej Kosec, Sergio P. Perez, and Andrew Fitzgibbon. Efficient sequence packing without cross-contamination: Accelerating large language models without impacting performance, 2022. URL <https://arxiv.org/abs/2107.02027>.
- [32] Kubernetes. Sidecar containers, 2024. URL <https://kubernetes.io/docs/concepts/workloads/pods/sidecar-containers/>. Kubernetes Documentation v1.29.
- [33] Conglong Li, Minjia Zhang, and Yuxiong He. The stability-efficiency dilemma: Investigating sequence length warmup for training gpt models, 2022. URL <https://arxiv.org/abs/2108.06084>.

- [34] Shen Li, Yanli Zhao, Rohan Varma, Omkar Salpekar, Pieter Noordhuis, Teng Li, Adam Paszke, Jeff Smith, Brian Vaughan, Pritam Damania, and Soumith Chintala. Pytorch distributed: Experiences on accelerating data parallel training, 2020. URL <https://arxiv.org/abs/2006.15704>.
- [35] Shen Li, Yanli Zhao, Rohan Varma, Omkar Salpekar, Pieter Noordhuis, Teng Li, Adam Paszke, Jeff Smith, Brian Vaughan, Pritam Damania, et al. Pytorch distributed: Experiences on accelerating data parallel training. *arXiv preprint arXiv:2006.15704*, 2020.
- [36] Bin Lin, Chen Zhang, Tao Peng, Hanyu Zhao, Wencong Xiao, Minmin Sun, Anmin Liu, Zhipeng Zhang, Lanbo Li, Xiafei Qiu, Shen Li, Zhigang Ji, Tao Xie, Yong Li, and Wei Lin. Infinite-llm: Efficient llm service for long context with distattention and distributed kvcache, 2024. URL <https://arxiv.org/abs/2401.02669>.
- [37] Hao Liu, Matei Zaharia, and Pieter Abbeel. Ring attention with blockwise transformers for near-infinite context, 2023.
- [38] Frank Sifei Luan, Ziming Mao, Ron Yifeng Wang, Charlotte Lin, Amog Kamsetty, Hao Chen, Cheng Su, Balaji Veeramani, Scott Lee, SangBin Cho, Clark Zinzow, Eric Liang, Ion Stoica, and Stephanie Wang. The streaming batch model for efficient and fault-tolerant heterogeneous execution, 2025. URL <https://arxiv.org/abs/2501.12407>.
- [39] Meta AI. The llama 4 herd: The beginning of a new era of natively multimodal ai innovation, April 2025. URL <https://ai.meta.com/blog/llama-4-multimodal-intelligence/>. Accessed: 2025-04-06.
- [40] Philipp Moritz, Robert Nishihara, Stephanie Wang, Alexey Tumanov, Richard Liaw, Eric Liang, Melih Elibol, Zongheng Yang, William Paul, Michael I. Jordan, and Ion Stoica. Ray: a distributed framework for emerging ai applications. In *Proceedings of the 13th USENIX Conference on Operating Systems Design and Implementation*, OSDI’18, page 561–577, USA, 2018. USENIX Association. ISBN 9781931971478.
- [41] Derek G. Murray, Jiri Simsa, Ana Klimovic, and Ihor Indyk. tf.data: A machine learning data processing framework, 2021. URL <https://arxiv.org/abs/2101.12127>.
- [42] Deepak Narayanan, Aaron Harlap, Amar Phanishayee, Vivek Seshadri, Nikhil R Devanur, Gregory R Ganger, Phillip B Gibbons, and Matei Zaharia. Pipedream: Generalized pipeline parallelism for dnn training. In *Proceedings of the 27th ACM symposium on operating systems principles*, pages 1–15, 2019.
- [43] Deepak Narayanan, Mohammad Shoeybi, Jared Casper, Patrick LeGresley, Mostofa Patwary, Vijay Korthikanti, Dmitri Vainbrand, Prethvi Kashinkunti, Julie Bernauer, Bryan Catanzaro, et al. Efficient large-scale language model training on gpu clusters using megatron-lm. In *Proceedings of the International Conference for High Performance Computing, Networking, Storage and Analysis*, pages 1–15, 2021.
- [44] PyTorch contributors. torch.utils.data — PyTorch 2.4 documentation, 2024. URL <https://pytorch.org/docs/stable/data.html>. Accessed: [Insert access date].
- [45] Jeff Rasley, Samyam Rajbhandari, Olatunji Ruwase, and Yuxiong He. Deepspeed: System optimizations enable training deep learning models with over 100 billion parameters. In *Proceedings of the 26th ACM SIGKDD International Conference on Knowledge Discovery & Data Mining*, pages 3505–3506, 2020.
- [46] Christoph Schuhmann, Richard Vencu, Romain Beaumont, Robert Kaczmarczyk, Clayton Mullis, Aarush Katta, Theo Coombes, Jenia Jitsev, and Aran Komatsuzaki. Laion-400m: Open dataset of clip-filtered 400 million image-text pairs. *arXiv preprint arXiv:2111.02114*, 2021.
- [47] John Schulman, Filip Wolski, Prafulla Dhariwal, Alec Radford, and Oleg Klimov. Proximal policy optimization algorithms. *arXiv preprint arXiv:1707.06347*, 2017.
- [48] Alexander Sergeev and Mike Del Balso. Horovod: fast and easy distributed deep learning in tensorflow, 2018. URL <https://arxiv.org/abs/1802.05799>.
- [49] Mohammad Shoeybi, Mostofa Patwary, Raul Puri, Patrick LeGresley, Jared Casper, and Bryan Catanzaro. Megatron-lm: Training multi-billion parameter language models using model parallelism. *arXiv preprint arXiv:1909.08053*, 2019.
- [50] Petru Soviany, Radu Tudor Ionescu, Paolo Rota, and Nicu Sebe. Curriculum learning: A survey, 2022. URL <https://arxiv.org/abs/2101.10382>.

- [51] Gemini Team, Rohan Anil, Sebastian Borgeaud, Jean-Baptiste Alayrac, Jiahui Yu, Radu Soricut, Johan Schalkwyk, Andrew M Dai, Anja Hauth, Katie Millican, et al. Gemini: a family of highly capable multimodal models. arXiv preprint arXiv:2312.11805, 2023.
- [52] Taegeon Um, Byungsoo Oh, Byeongchan Seo, Minhyeok Kweun, Goeun Kim, and Woo-Yeon Lee. Fastflow: Accelerating deep learning model training with smart offloading of input data pipeline. Proc. VLDB Endow., 16(5):1086–1099, jan 2023.
- [53] P Umesh. Image processing in python. CSI Communications, 23, 2012.
- [54] Ashish Vaswani, Noam Shazeer, Niki Parmar, Jakob Uszkoreit, Llion Jones, Aidan N. Gomez, Lukasz Kaiser, and Illia Polosukhin. Attention is all you need, 2023. URL <https://arxiv.org/abs/1706.03762>.
- [55] Marcel Wagenländer, Guo Li, Bo Zhao, Luo Mai, and Peter Pietzuch. Tenplex: Dynamic parallelism for deep learning using parallelizable tensor collections. In Proceedings of the ACM SIGOPS 30th Symposium on Operating Systems Principles, pages 195–210, 2024.
- [56] Borui Wan, Mingji Han, Yiyao Sheng, Zhichao Lai, Mofan Zhang, Junda Zhang, Yanghua Peng, Haibin Lin, Xin Liu, and Chuan Wu. Bytecheckpoint: A unified checkpointing system for llm development, 2024. URL <https://arxiv.org/abs/2407.20143>.
- [57] Peng Wang, Shuai Bai, Sinan Tan, Shijie Wang, Zhihao Fan, Jinze Bai, Keqin Chen, Xuejing Liu, Jialin Wang, Wenbin Ge, Yang Fan, Kai Dang, Mengfei Du, Xuancheng Ren, Rui Men, Dayiheng Liu, Chang Zhou, Jingren Zhou, and Junyang Lin. Qwen2-vl: Enhancing vision-language model’s perception of the world at any resolution, 2024. URL <https://arxiv.org/abs/2409.12191>.
- [58] Chengyue Wu, Xiaokang Chen, Zhiyu Wu, Yiyang Ma, Xingchao Liu, Zizheng Pan, Wen Liu, Zhenda Xie, Xingkai Yu, Chong Ruan, and Ping Luo. Janus: Decoupling visual encoding for unified multimodal understanding and generation, 2024. URL <https://arxiv.org/abs/2410.13848>.
- [59] Zhiyu Wu, Xiaokang Chen, Zizheng Pan, Xingchao Liu, Wen Liu, Damai Dai, Huazuo Gao, Yiyang Ma, Chengyue Wu, Bingxuan Wang, Zhenda Xie, Yu Wu, Kai Hu, Jiawei Wang, Yaofeng Sun, Yukun Li, Yishi Piao, Kang Guan, Aixin Liu, Xin Xie, Yuxiang You, Kai Dong, Xingkai Yu, Haowei Zhang, Liang Zhao, Yisong Wang, and Chong Ruan. Deepseek-vl2: Mixture-of-experts vision-language models for advanced multimodal understanding, 2024. URL <https://arxiv.org/abs/2412.10302>.
- [60] Jiasheng Ye, Peiju Liu, Tianxiang Sun, Yunhua Zhou, Jun Zhan, and Xipeng Qiu. Data mixing laws: Optimizing data mixtures by predicting language modeling performance, 2024. URL <https://arxiv.org/abs/2403.16952>.
- [61] Xinyu Zeng, Yulong Hui, Jiahong Shen, Andrew Pavlo, Wes McKinney, and Huanchen Zhang. An empirical evaluation of columnar storage formats. Proc. VLDB Endow., 17(2):148–161, October 2023. doi: 10.14778/3626292.3626298.
- [62] Zili Zhang, Yinmin Zhong, Ranchen Ming, Hanpeng Hu, Jianjian Sun, Zheng Ge, Yibo Zhu, and Xin Jin. Disttrain: Addressing model and data heterogeneity with disaggregated training for multimodal large language models. arXiv e-prints, pages arXiv–2408, 2024.
- [63] Mark Zhao, Niket Agarwal, Aarti Basant, Buğra Gedik, Satadru Pan, Mustafa Ozdal, Rakesh Komuravelli, Jerry Pan, Tianshu Bao, Haowei Lu, Sundaram Narayanan, Jack Langman, Kevin Wilfong, Harsha Rastogi, Carole-Jean Wu, Christos Kozyrakis, and Parik Pol. Understanding data storage and ingestion for large-scale deep recommendation model training: industrial product. In Proceedings of the 49th Annual International Symposium on Computer Architecture, ISCA ’22. ACM, June 2022. URL <http://dx.doi.org/10.1145/3470496.3533044>.
- [64] Mark Zhao, Emanuel Adamiak, and Christos Kozyrakis. cedar: Optimized and unified machine learning input data pipelines. arXiv preprint arXiv:2401.08895, 2024.
- [65] Yanli Zhao, Andrew Gu, Rohan Varma, Liang Luo, Chien-Chin Huang, Min Xu, Less Wright, Hamid Shojanazeri, Myle Ott, Sam Shleifer, et al. Pytorch fsdp: experiences on scaling fully sharded data parallel. arXiv preprint arXiv:2304.11277, 2023.
- [66] Yu Zhu, Wenqi Jiang, and Gustavo Alonso. Multi-tenant smartnics for in-network preprocessing of recommender systems, 2025. URL <https://arxiv.org/abs/2501.12032>.

Appendix

A Ablation Study on Parallelism Redundancy Removal

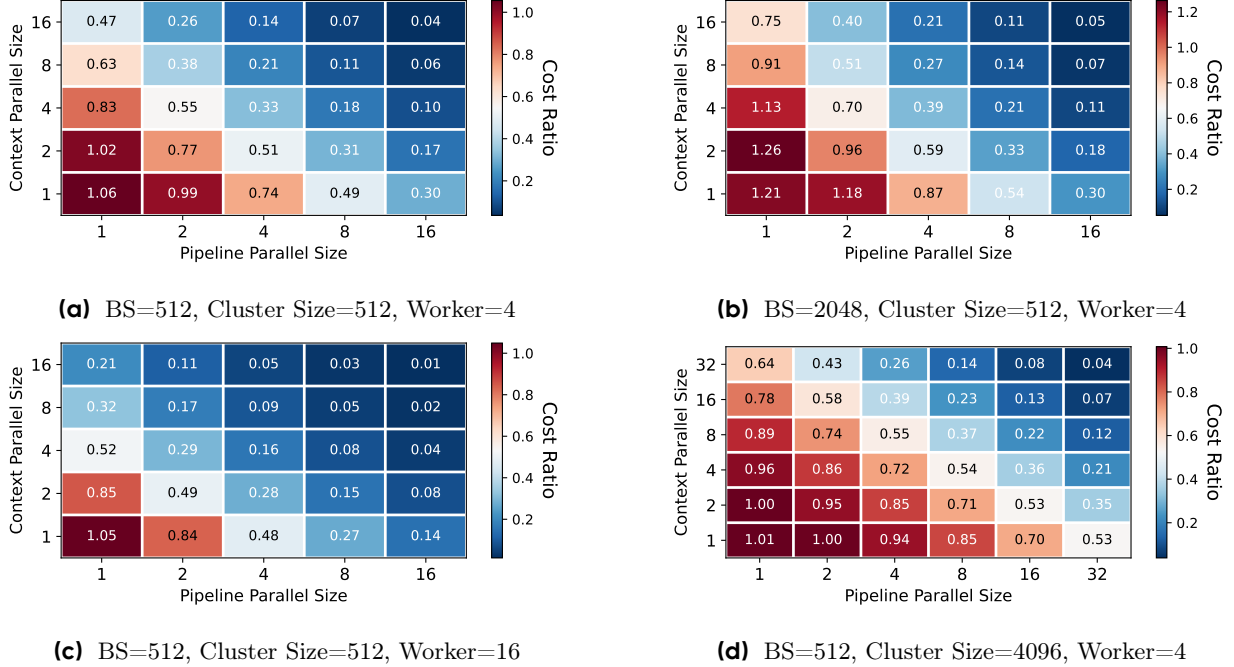


Figure 17 Ablation study of cluster and training parameters on read amplification costs.

We conduct an ablation study on three additional parameters related to read amplification using our cost model: batch size, worker count, and cluster size. Specifically, we vary the original setup (batch size = 512, worker count = 4, cluster size = 512) to a modified configuration (batch size = 2048, worker count = 16, cluster size = 4096) to characterize their effects.

As shown in Fig. 17b, increasing the batch size elevates the memory cost of OVERLORD. This arises because the data constructor introduces additional buffer storage for data and communication, whose overhead scales with the data size. Conversely, a larger worker count exacerbates loader redundancy (Fig. 17a), making the cost savings from redundancy reduction more pronounced. For cluster size, when parallelism granularity (context parallelism (CP), pipeline parallelism (PP)) is small, a larger cluster increases the effective DP size, making it harder for OVERLORD to reduce memory costs when data constructors are active and loader redundancy is low. However, larger clusters enable higher-degree parallelism—common practice for scaling models with increased PP or CP—which ensures OVERLORD remains cost-efficient in such scenarios.

B Scalability Advantages of the Actor Model

We evaluated OVERLORD against a baseline system that employs direct data transfer from Source Loaders to Trainers (with the Data Constructor disabled). At smaller scales (e.g., 1k GPUs), activating the Data Constructor yields modest performance improvements over the baseline. As the system scales to 2k GPUs, however, the Data Constructor significantly mitigates connection overhead. Notably, we measure a $10\times$ increase in data fetch latency for the baseline compared to OVERLORD. At 4k GPUs, the baseline system collapses due to communication bottlenecks, unable to sustain training progress, while OVERLORD maintains throughput via data redistribution. These results highlight the critical role of the Data Constructor for extreme-scale workloads.

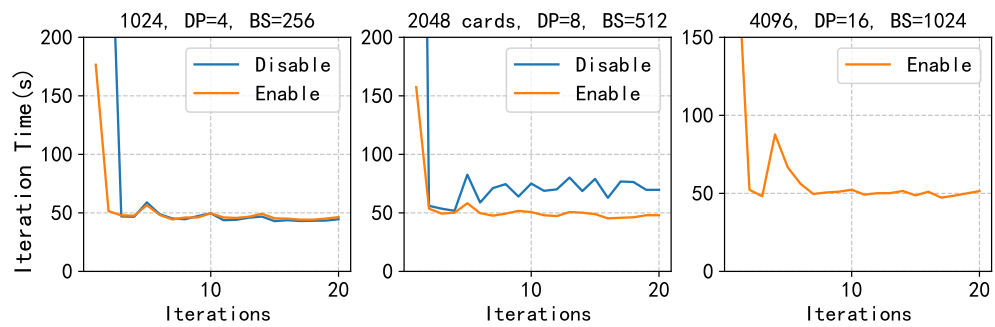


Figure 18 Large Scale Evaluation w.r.t. Data Constructor.